

# Electronic Correlation and Transport Properties of Nuclear Fuel Materials

Quan Yin, Andrey Kutepov, Kristjan Haule, and Gabriel Kotliar  
*Department of Physics and Astronomy, Rutgers University, Piscataway, NJ 08854*

Sergey Y. Savrasov and Warren E. Pickett  
*Department of Physics, University of California, Davis, CA 95616*  
 (Dated: November 18, 2010)

Actinide elements, such as uranium and plutonium, and their compounds are best known as nuclear materials. When engineering optimal fuel materials for nuclear power, important thermophysical properties to be considered are melting point and thermal conductivity. Uranium and plutonium oxide fuels used in very high temperature fast breeder reactors suffer from poor thermal conductivity, because in these insulating oxides only lattice vibrations conduct heat. Hence attention is turning to metallic fuels, such as uranium carbide and nitride, for the generation IV advanced nuclear reactors [1]. Understanding the physics underlying transport phenomena due to electrons and lattice vibrations in actinide systems is a crucial step toward the design of better fuels. This has been a challenging theoretical problem because of the competition between itinerancy and localization of the valence  $5f$ -electrons and the multiplicity of mechanisms governing the charge and heat transport. Using modern first-principle computational methods, we survey the landscape of nuclear fuel materials among binary compounds. We find that different mechanisms, electrons–electron and electron–phonon interactions, are responsible for the transport in the uranium nitride and carbide. Our findings allow us to make predictions on how to improve their thermal conductivities.

Here we argue that both electron–electron and electron–lattice interactions need to be accounted for in the design of nuclear fuel materials with desired transport characteristics. According to the Lindemann criterion, solids with large Debye frequencies have high melting points. This is typically found in insulators where atomic bonds are strong due to lack of electronic screening. On the other hand, high thermal conductivity can usually be achieved in metals where conduction electrons are dominant heat carriers. Searching for the desired fuel material is to balance the above two conditions. Applying these principles to the actinide compounds leads us to an observation that systems close to the Mott transition from the metallic side are the best option. We start by concentrating on the class of actinide oxides, nitrides and carbides based on uranium, neptunium, plutonium, americium and curium. Probing the proximity to the

metal–insulator transition through their electronic structures and its effect on the two scattering processes, is the central task of the present work.

Thermophysical properties of solids are determined from their electronic structures, but in actinides they are not well described by the traditional approaches based on density functional theory (DFT) within its local density approximation (LDA) due to strong electronic correlation. Thus it requires a theory that can take into account both itinerant and localized behaviors of the correlated electrons on equal footing. In this study we use an advanced electronic structure method based on the combination of LDA and dynamical mean field theory (LDA+DMFT) [2], which has proven success in describing such strongly correlated problem [3–6]. We use the full-potential charge self-consistent implementation of LDA+DMFT described in Ref.[8] based on the DFT program of Ref.[7]. At the heart of the DMFT method is the numeric solution of the Anderson quantum impurity model, which is here achieved by the continuous time quantum Monte Carlo (CTQMC) algorithm [9, 10]. For late actinides such as Pu and beyond, we use the less expensive vertex corrected one-crossing approximation (OCA) [2], which is very accurate in these more localized systems. All calculations were performed in the paramagnetic phase.

We first describe the chemical trends governing the degree of localization of the  $f$ -electrons in the binary

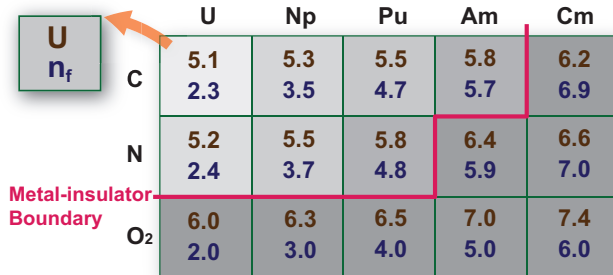


FIG. 1. **Correlation diagram.** The shading represents the electronic correlation strength. The labels on the top denote the actinides elements, and the labels to the left denote the ligand elements. The red line is the metal–insulator boundary. Two quantities are listed in each cell: Hubbard  $U$  (units: eV) and  $f$ -electron valence  $n_f$ .

actinide compounds listed in Fig. 1. The key parameters are: the onsite Coulomb repulsion among the  $5f$ -electrons, quantified by the Hubbard  $U$  and Hund's rule exchange  $J$ ; the charge transfer energy  $\Delta = \varepsilon_f - \varepsilon_p$ ; and the  $5f$  band width quantified by the hybridization between  $5f$  and  $spd$  electrons. The charge transfer energy increases vertically from carbides to oxides due to the change in the electro-negativity of ligand atoms. The band width of  $5f$ -electrons shrinks horizontally from U to Cm compounds, indicating a more localized nature in late actinides. This causes a reduction of screening which is manifest in the gradual increase of  $U$  from the left to the right, and from the top to the bottom of the table.

While most electronic structure methods can accurately calculate the hopping integrals between various electronic orbitals, evaluating the screened  $U$  in solids is generally a difficult task. Here we have computed  $U$  using a newly developed fully self-consistent many-body GW approach [11], which provides a seamless interface with LDA+DMFT. The latter method allows to determine the degree of localization of the  $5f$ -electrons in each material. Our estimates for the Hund's  $J$  are within the range of  $0.5 - 0.6$  eV, about 30% smaller than their atomic values due electronic screening. As a combination of the above quantities, the overall correlation strength and localization is visualized by the shading of Fig. 1, referred as the "correlation diagram" of binary nuclear fuel materials, where the gray gradient approximately represents the partial  $f$  density of states at the Fermi level computed by LDA+DMFT.

Next, we present the frequency dependence of the electronic spectral functions of some representative compounds in Fig. 2(a). From the top panel to the bottom, the  $5f$  partial DOS changes qualitatively. UC and UN represent an itinerant  $5f$ -electron system with most spectral weight on the Fermi level, but the picture starts to change at PuN, where the Kondo resonance and satellite  $5f$  states are present. In AmN the  $5f$  DOS begins to form an marginal energy gap. The evolution of the density of states from UN to CmN echoes the itinerancy-localization transition of  $5f$ -electrons, and demonstrates the metal-insulator transition in a transparent point of view. CmC, CmN, and all the actinide oxides are also found to be insulators. This allows to establish a metal-insulator transition boundary, illustrated by the red line in Fig. 1.

The actinides ions in most of the metallic crystals are found to be in a mixed valence state, where they do not settle in one valence, but fluctuate between different valences in the solid. It can be described by an effective number  $n_f$  (listed in Fig. 1), obtained using a valence histogram technique [5], which represents an average over all the atomic configurations weighted by corresponding probabilities.

The total and partial DOS of  $\text{UO}_2$  and  $\text{PuO}_2$  are shown in Fig. 2(b) and 2(c). Most noticeably, the situation

$U > \Delta$  allows us to describe the insulating actinide oxides as charge transfer Mott-insulators [12], which is well known from late transition metal oxides, for example NiO, the classical textbook example of strongly correlated systems. Thus they could exhibit the Zhang-Rice state (ZRS) [13], which is the low-energy resonance corresponding to the coupling of local moments of correlated electron orbitals to the hole induced by phototemission process on ligand orbitals. The appearance of the ZRS in  $\text{UO}_2$  can be understood from the existence of a local magnetic moment in the U  $5f^2$  many-body ground state, which is the  $\Gamma_5$  triplet. It is also clear that  $\text{PuO}_2$  does not show the ZRS because its ground state of the  $5f^4$ -shell is the  $\Gamma_1$  singlet.

After understanding the electronic structures, we turn to the transport properties. We focus on correlated metallic compounds, where electrons play the role of charge and heat transporters, while retaining a high melting point. Although in normal metals electron-phonon scattering is dominant except at very low temperatures, in strongly correlated metals electron-electron scattering takes the lead. The electronic contribution to thermal conductivity is proportional to the electrical conductivity via the Wiedemann-Franz law. From the electronic structure and correlation strength of the studied materials, small resistivity occurs in the least correlated compounds in our table. Indeed UC and UN are the best fuel materials in terms of their outstanding transport prop-

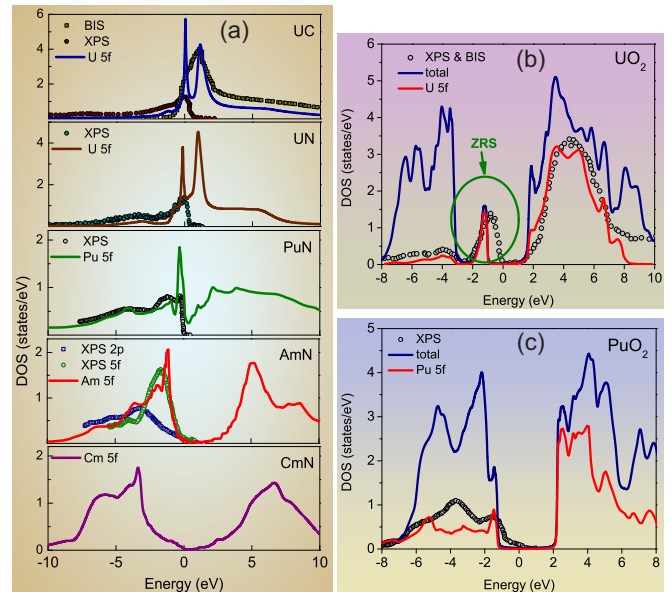


FIG. 2. **Theoretical DOS compared with available x-ray photoemission spectroscopy.** (a) Partial  $5f$  DOS of UC and select actinide nitrides. The XPS & BIS data of UC is from Ref.[14], UN from Ref.[15], PuN from Ref.[19], and AmN from Ref.[18]. (b) Total and partial DOS of  $\text{UO}_2$ . XPS and BIS taken from Ref.[16]. (c) Total and partial DOS of  $\text{PuO}_2$ . XPS from Ref.[17].

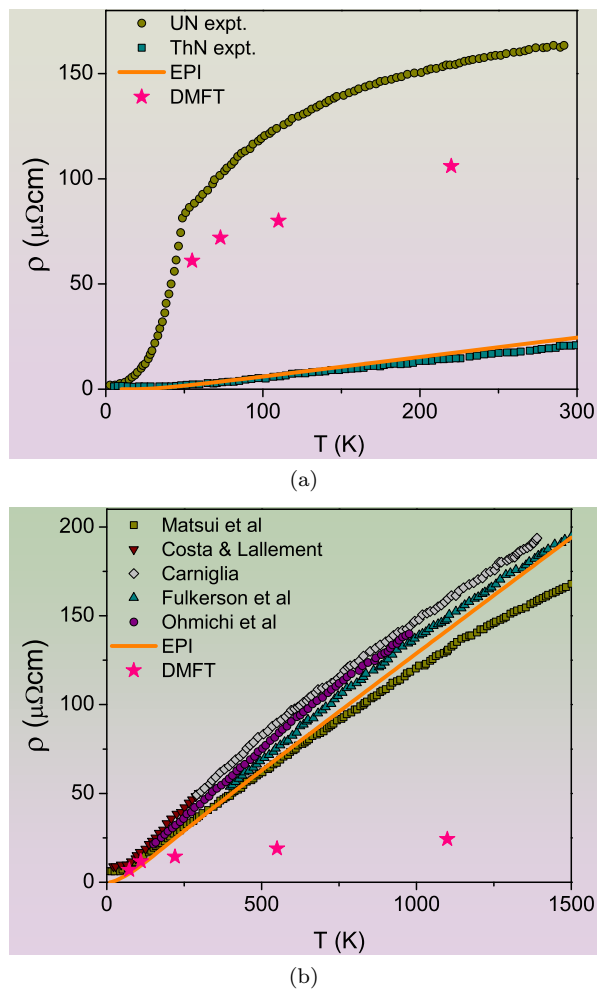


FIG. 3. **Electrical resistivity due to two different scattering mechanisms.** The electron–phonon interaction (EPI) resistivity is shown as solid lines, and electron–electron interaction resistivity, which is calculated by LDA+DMFT (CTQMC) at several temperatures, is shown as stars. (a) UN. Experimental resistivity data are taken from Ref.[15]. (b) UC. Experimental data after Ref.[23–27].

erties.

Strong Coulomb interactions among electrons can substantially reduce the interaction between electrons and lattice vibrations [21]. Hence the electron–phonon interaction (EPI) is usually weaker in strongly correlated materials, leading to smaller resistivity due to EPI. On the other hand, increasing electronic correlations leads to an increase in resistivity due to electron–electron scattering. Therefore neither extremely weak nor strong correlations is good from the perspective of minimizing resistivity. Deciding the optimal degree of correlation for the purpose of maximizing conductivity thus requires first-principle calculations.

Experimentally, UC is a Fermi liquid (FL) at room temperature and ARPES measurement indicates that the overall band width is reduced by a factor of 4 relative to

the LDA band structure [20]. In our calculation UC is a FL below 300K with  $m^*/m_{LDA} = 3.7$ . On the other hand, UN shows a strongly correlated heavy fermion character with a coherence temperature below its Neel temperature of 53K. In the absence of magnetic order, UN would be a FL at very low temperature with a large mass enhancement ( $m^*/m_{LDA} \approx 12$ ) as can be inferred from the linear specific heat coefficient [28]. It is a non FL in the temperature range (55 – 1000K) we studied.

To evaluate the conductivity due to electron–electron scattering we use the Kubo formalism [8], where the scattering rate comes from the imaginary part of DMFT self-energy  $\Sigma(\omega, T)$ , obtained from CTQMC.

The effect of electron–phonon scattering was evaluated using a generalized linear response method for strongly correlated systems, where a two-pole interpolation was used to approximate the self-energy obtained from CTQMC. This accounts for both the strong quasi-particle renormalization of correlated electrons at the Fermi surface, and their spectral weight transfer to higher energies. Based on the phonon data computed by the density functional linear–response approach, we evaluate electron–phonon contributions to electrical and thermal resistivity by solving the Boltzmann equation.

We can now build the entire picture of the electronic transport in the uranium compounds with our results summarized in Fig. 3. Electron–electron scattering can account for approximately 80% of  $\rho(T)$  in UN, commonly found in heavy fermion systems, entitling it as a strongly correlated bad metal. In contrast, UC shows nearly linear  $\rho(T)$ , which is an indication of dominant electron–phonon scattering, and our calculated results indeed show that in UC,  $\rho(T)_{ee}$  is much smaller than  $\rho(T)_{EPI}$ . Our findings verify the distinct characters in the electrical transport of UC and UN, two seemingly similar materials. By making a side–to–side comparison, we see that UC is less correlated than UN, which makes  $\rho(T)_{ee}$  larger in the latter. Nevertheless  $\rho(T)_{EPI}$  is larger in the former. The difference in  $\rho(T)_{EPI}$  can be ascribed to the distinction in the Fermi surfaces of UC and UN. The nitride has one more valence electron than the carbide, which changes the topology and pockets size of the Fermi surface, as well as the average electron velocity  $v_F$ . This results in a factor of 10 difference in the electron–phonon coupling constant  $\lambda$  between UC and UN. Similar situation has been known in many transition metals, both theoretically and experimentally [22].

While electrical current can only be carried by electrons in solids, excitations other than electrons may contribute to thermal conductivity. Here we also estimate lattice vibrational contribution to thermal conductivity in UC and UN. This is done by evaluating the Gruneisen parameter and phonon group velocities using the method described previously for MOX fuels [6]. According to our result, at  $T = 1000K$ , lattice thermal conductivity  $\kappa_{ph}$  is equal to  $2.7W/mK$  in UC, and  $\kappa_{ph} = 4.4W/mK$  in UN.

Thus  $\kappa_{ph}$  only plays a minor role in these two metallic uranium compounds.

We put together our results and evaluate total thermal conductivity at  $1000K$ , a representative temperature under which nuclear reactors operate. By applying the Wiedemann–Franz law on the electrical conductivity data, we obtain  $\kappa_{ee}$ . Since electronic thermal resistivity consists of two scattering processes, total thermal conductivity is estimated by  $\kappa_{total} = (\kappa_{ee}^{-1} + \kappa_{EPI}^{-1})^{-1} + \kappa_{ph}$ , in which the first two terms correspond to  $\kappa_{electron}$ . For UN, our result is  $\kappa_{total} = 16.5W/mK$ , compares well with a recent study which extracted the phonon contribution from molecular dynamics (MD)[29] and the electronic contribution from experiments. Experimentally,  $\kappa(1000K) \approx 19 - 23W/mK$ . In UC, we obtained  $\kappa_{total} = 18.7W/mK$ , also close to the experimental value of  $23W/mK$  [30]. The discrepancy between theory and experiment is likely due to other excitations that can conduct heat and are not accounted for in our calculation, and the approximate nature of the Wiedemann Franz law and Boltzmann transport theory which are used to obtain the electronic and lattice thermal conductivity, respectively.

Most importantly, the understanding gained from our computational study suggests avenues for improving the thermal conductivity of UC and UN. Since optimizing thermal conductivity is equivalent to minimizing resistivity at high temperatures, it is interesting to look at the doping dependence of the resistivity in UC/UN, or in the solid solution  $UC_{1-x}N_x$ . Let us represent the total resistivity of  $UC_{1-x}N_x$  by  $\rho(T, x) = \rho(T, x)_{ee} + \rho(T, x)_{EPI}$ . Note that on one hand,  $\rho(T, x)_{ee}$  should show a rapid growth when  $x$  approaches 1 since  $\rho(T)_{ee} \propto 1/T_K \propto W/Z$  above coherence temperature, where  $T_K$  is the Kondo temperature and  $W$  is the band width. On the other hand,  $\rho(T, x)_{EPI}$  being proportional to transport coupling constant  $\lambda_{tr}$  divided by the average square of the Fermi velocity  $N(0)\langle v^2 \rangle$  of the quasiparticles decreases with  $x$  in our calculation. Therefore there exists a region between UC and UN where the total resistivity is minimized. It is also possible to achieve similar effects in UC by electron doping, or in UN by hole doping.

To conclude, we have carried out the first LDA+DMFT exploration of the electronic structure and transport properties of nuclear fuels. The actinide dioxides are charge–transfer insulators, where the Zhang–Rice state is present in  $UO_2$ . The metallic carbide and nitride compounds exhibit strong electronic correlations, which is reflected in the incoherent non Fermi liquid behavior at temperatures relevant for nuclear reactions. We have achieved a successful theoretical description of the transport in UC and UN, two of the most promising fuel materials due to their excellent thermophysical properties. While UN clearly shows a strongly correlated signature, both the electron–electron and electron–phonon scattering mechanisms contribute

to transport in the less correlated sister compound UC. Finally, our findings enable us to give predictions on how to improve these two uranium based nuclear fuel materials.

- 
- [1] Butler, D. Energy: Nuclear power’s new dawn. *Nature* **429**, 238 (2004).
  - [2] Kotliar, G. et al. Electronic structure calculations with dynamical mean-field theory. *Rev. Mod. Phys.* **78**, 856 (2006).
  - [3] Savrasov, S. Y., Kotliar, G. & Abrahams, E. Correlated electrons in  $\delta$ -plutonium within a dynamical mean-field picture. *Nature* **410**, 793 (2001).
  - [4] Dai, X. et al. Calculated Phonon Spectra of Plutonium at High Temperatures. *Science* **300**, 953 (2003).
  - [5] Shim, J. H., Haule, K. & Kotliar, G. Fluctuating valence in a correlated solid and the anomalous properties of  $\delta$ -plutonium, *Nature* **446**, 513 (2007).
  - [6] Yin, Q. & Savrasov, S. Y. Origin of Low Thermal Conductivity in Nuclear Fuels. *Phys. Rev. Lett.* **100**, 225504 (2008).
  - [7] Blaha, P. K., Schwarz, K., Madsen, G., Kvasnicka, D. & Luitz, J. WIEN2K package, <http://www.wien2k.at>.
  - [8] Haule, K., Yee, C-H & Kim, K. Dynamical mean-field theory within the full-potential methods: Electronic structure of  $CeIrIn_5$ ,  $CeCoIn_5$ , and  $CeRhIn_5$ . *Phys. Rev. B* **81**, 195107 (2010).
  - [9] Haule, K. Quantum Monte Carlo impurity solver for cluster dynamical mean-field theory and electronic structure calculations with adjustable cluster base. *Phys. Rev. B* **75**, 155113 (2007).
  - [10] Werner, P., Comanac, A., de Medici, L., Troyer, M. & Millis, A. J. Continuous-Time Solver for Quantum Impurity Models. *Phys. Rev. Lett.* **97**, 076405 (2006).
  - [11] Kutepov, A., Haule, K., Savrasov, S. Y. and & Kotliar, G. Self-consistent GW determination of the interaction strength: Application to the iron arsenide superconductors. *Phys. Rev. B* **82**, 045105 (2010).
  - [12] Zaanen, J., Sawatzky, G. A. & Allen, J. W. Band gaps and electronic structure of transition-metal compounds. *Phys. Rev. Lett.* **55**, 418 (1985).
  - [13] Zhang, F. C. & Rice, T. M. Effective Hamiltonian for the superconducting Cu oxides. *Phys. Rev. B* **37**, 3759 (1988).
  - [14] Ejima, T et al. Electronic structure of UC studied by X-ray photoemission and bremsstrahlung isochromat spectroscopy. *Physica B* **186-188**, 77 (1993).
  - [15] Samsel-Czekala, M. et al. Electronic structure and magnetic and transport properties of single-crystalline UN. *Phys. Rev. B* **76**, 144426 (2007).
  - [16] Baer, Y. & Schoenes, J. Electronic structure and Coulomb correlation energy in  $UO_2$  single crystal. *Solid State Communication* **33**, 885 (1980).
  - [17] Butterfield, M. T. et al. Photoemission of surface oxides and hydrides of delta plutonium. *Surface Science* **571**, 74 (2004).
  - [18] Gouder, T., Oppeneer, P. M., Huber, F., Wastin, F. & Rebizant, J. Photoemission study of the electronic structure of Am, AmN, AmSb, and  $Am_2O_3$  films. *Phys. Rev. B* **72**, 115122 (2005).

- [19] Havelaet, L., Wastin, F., Rebizant, J. & Gouder, T. Photoelectron spectroscopy study of PuN. *Phys. Rev. B* **68**, 085101 (2003).
- [20] Ito, T., et al. Electronic structure and Fermi surface of UC studied by high-resolution angle-resolved photoemission spectroscopy. *Journal of Magnetism and Magnetic Materials* **226-230**, 40 (2001).
- [21] Gunnarsson, O., & Rösch, O. Interplay between electron-phonon and Coulomb interactions in cuprates. *J. Phys.: Condens. Matter* **20**, 043201 (2008).
- [22] Butler, W. H. Electron-phonon coupling in the transition metals: Electronic aspects. *Phys. Rev. B* **15**, 5267 (1977).
- [23] Matsui, H., Tamaki, M., Nasu, S. & Kurasawa, T. Electrical resistivities of the uranium carbides. *J. Phys. Chem. Solids* **41**, 351 (1980).
- [24] Costa, P. & Lallement, R. Resistive et pouvoir thermo-electrique des carbures de thorium, d'uranium et de plutonium. *Phys. Lett.* **7**, 21 (1973).
- [25] Carniglia, S. Carbides in Nuclear Energy (Edited by L. Russell et al), Vol. **1**, p.365. Macmillan, London (1964).
- [26] Fulkerson, W. et al. Pu 1970 and Other Actinides (Edited by W. Miner), Part 2, p.374. Jack V. Richard Executive Publisher (1970).
- [27] Ohmichi, T., Kikuchi, T., & Nasu, S. J. Electrical Resistivity and Thermoelectric Power of  $UC_{1-x}N_x$ . *Nucl. Sci. Tech.* **9**, 77 (1972).
- [28] Yoshizawa, M. & Suzuki, T. Thermal and elastic properties of UN. *Journal of Magnetism and Magnetic Materials* **90 & 91**, 523, (1990).
- [29] Kurosaki, K., Yano, K., Yamada, K., Uno, M. & Yamanaka, S. A molecular dynamics study of the thermal conductivity of uranium mononitride. *Journal of Alloys and Compounds* **311**, 305 (2000).
- [30] De Coninck, R., Van Lierde, W. & Gijs, A. Uranium carbide: Thermal diffusivity, thermal conductivity and spectral emissivity at high temperatures. *Journal of Nuclear Materials*, **57**, 69 (1975).

**Acknowledgements** This work is supported by the United States Department of Energy Nuclear Energy University Program, contract No. 00088708. WEP acknowledges DOE Grant NO. DE-FG02-04ER46111. We acknowledge the support of Computational Materials Science Network, Grant NO. DE-FG03-01ER45876, and Grant NO. DE-SC0005468 linking UC Davis and Rutgers. QY thanks Viktor Oudovenko at Rutgers University for technical support on computation.

**Author information** Correspondence and requests for materials should be addressed to Quan Yin. Email address: leoquan@gmail.com